

Article

# Chattering Free Adaptive Sliding Mode Controller for Photovoltaic Panels with Maximum Power Point Tracking <sup>†</sup>

Hina Gohar Ali <sup>1,2,\*</sup>  and Ramon Vilanova Arbos <sup>1</sup> 

<sup>1</sup> Department Telecommunications and Systems Engineering, School of Engineering, Universitat Autònoma de Barcelona, Bellaterra, 08193 Cerdanyola del Vallés, Barcelona, Spain; ramon.vilanova@uab.cat

<sup>2</sup> School of Electrical Engineering and Computer Science, National University of Sciences and Technology (NUST), Islamabad 44000, Pakistan

\* Correspondence: hina.goharali@e-campus.uab.cat

<sup>†</sup> This paper is an extended version of our paper published in 2020 IEEE 20th International Conference on Environmental and Electrical Engineering (EEEIC), Madrid, Spain, June 2020.

Received: 26 September 2020; Accepted: 28 October 2020; Published: 30 October 2020



**Abstract:** Photovoltaic system is utilized to generate energy that relies upon the ecological conditions, for example, temperature, irradiance, and the load associated with it. Considering the non-linear component of photovoltaic (PV) array and the issue of low effectiveness because of the variable natural conditions, the Maximum Power Point Tracking (MPPT) method is required to extract the maximum power from the PV system. The adopted control is executed utilizing an Adaptive Sliding Mode Controller (ASMC) and the enhancement is actualized utilizing an Improved Pattern Search Method (IPSM). This work employs IPSM based optimization approach in order to command the underlying ASMC controller. The upper level decision determines the sliding surface for the adaptive controller. As a non-linear strategy, the stability of the adaptive controller is guaranteed by conducting a Liapunov analysis. On the practical side, MATLAB/Simulink is used as simulator for the controller implementation and coupling with PSIM in order to connect it with the PV system object of control. The simulation results validate that the proposed controller effectively improves the voltage tracking, system power with reduced chattering effect and steady-state error. The performance of the proposed control architectures is validated by comparing the proposals with that of the well-known and widely used Proportional Integral Derivative (PID) controller. That operated as a lower level controller for a Perturb & Observe (P&O) and Particle Swarm Optimization (PSO).

**Keywords:** photovoltaic (PV); maximum power point tracking (MPPT); adaptive sliding mode controller (ASMC); improved pattern search method (IPSM); particle swarm optimization (PSO)

## 1. Introduction

Energy is currently recognized as the most demanded resource in our daily lives, being the essential part that determines the development of economy as well social growth. At the global level, energy crises are highly present, and can be reduced by the optimum utilization of sustainable energy. Solar energy is the most commonly available free energy renewable resource across the world, which is clean, sustainable, and environmentally friendly [1]. Photovoltaic technology is used to obtain electrical energy from solar energy by using PV panel. PV panel is made up of several PV solar cells in series and parallel combinations. The behavior of the desired PV output is of non-linear type. This is what makes its operation difficult. The main figure of interest is the Maximum Power Point (MPP) which can be altered because of variable environmental conditions (i.e., solar irradiance and temperature) at different operating points. The current-voltage (I-V) and power-voltage (P-V) characteristics will

also be altered because of such changing operating conditions. Therefore, to operate the PV system at particular MPP under the given meteorological conditions control strategies are needed to formulate in order to extract and deliver the maximum possible power from the PV which improves the overall efficiency of the PV system and minimize power losses.

The operation of the PV output characteristics in order to extract the MPP and maximize the PV operation benefits, a number of operation and control algorithms have been proposed in the literature. Such algorithms can be distinguished among them on the basis of features such as complexity, implementation, and speed of convergence, among others [2]. Generally, these algorithm techniques are divided into Conventional Techniques (CTs), Soft Computing Technique (SCTs), and linear and nonlinear control techniques [3].

In conventional algorithms, Perturb and Observe (P&O) [4] and Incremental Conductance (INC) [5] are the main basic algorithms. These proposed CTs are simple, easy in implementation and have the capacity of tracking the MPP efficiently at present ecological conditions, but the drawback of these CTs is the fluctuations around MPP, which influence the accuracy rapidity of the system, resulting in a loss of useful power [6].

Soft-computing based techniques have proven to be powerful to deal with the MPPT optimization problem as per comparison with the classical ones [7].

SCTs techniques consist of Artificial Intelligence Techniques (AITs) [8] and Bio-Inspired Techniques (BITs) [9]. Fuzzy logic controller [10], artificial neural network [11], and genetic algorithms [12] comes in the category of AITs. These methods require extensive high computation when dealing with the nonlinear characteristics of the I-V curves, although AITs methods are generally effective. Along with this, the PV system operating conditions change continuously with time; therefore, MPPT has to respond in real time to the environmental condition variations (insolation and temperature). Hence, a large memory size and computing requirements are usually required.

One of the features that characterize some of the BITs proposals that can be found in the literature is its ability for optimal searching in the search space but with moderate computational effort. These methods have the tendency to converge quickly to a global maximum; thus, they can save power loss even in a partially shaded environment. Cuckoo search algorithm [13], ant colony optimization [14], particle swarm optimization [15], and evolutionary algorithm [16] are the proposed latest techniques developed in the class of BITs. Despite their usefulness in various environmental conditions, these techniques are inefficient because their slow convergence obstructs their practical usage as on-line solutions.

Recently, a MPPT improvement approach dependent on Pattern Search was proposed in [17]. The strategy introduced depends on Generalized Pattern Search Method (GPSM). The GPSM was proposed in [18] for subsidiary free unconstrained enhancement of constantly differentiable convex function and has been utilized from that point forward in various control approaches. Hence, in this paper, the Improved Pattern Search Method (IPSM) optimization algorithm is used, which was introduced in [19].

The operational configuration can also be built up based upon linear controllers that will operate as voltage controllers, obeying the reference voltage generated by a suitable MPPT algorithm as well as trying to minimize the effect of environmental perturbations [20–22]. The linear controller option, however, needs a linear model to be designed. That linear model is usually a linearization of the non-linear PV model. As is well known, this representation may work well on the required operating point but loses representative power in other PV working range. As an alternative to the need of a linearized model, other controllers have been proposed. Most of those controllers, in order to guarantee good performance in all operating ranges, do include adaptive laws [23] and energy balance [24]. In the MPPT literature, different non-linear operation configurations can be found as good alternatives to deal with the non-linear dynamics of the PV as well as power converters [25].

The presented scenario has motivated the introduction of a Sliding-Mode Control MPPT (SMC-MPPT) as a robust controller because of the inherent robustness as well as the stability

characteristics of SMC controllers. In SMC-MPPT, the tracking error is considered as a sliding surface [26]. In SMC, the control scheme is intended to drive and, afterward, hold the system states within the limits of the switching function. It can be found in the literature that the SMC has been widely used as a good option for controlling non-linear processes. Among them, DC–DC converters that operate in PV systems [27]. Two-loop MPPT control approaches were tended to in [28,29], which require either a current reference or voltage reference. This control approach based on terminal sliding mode control. The chattering was addressed in [30,31], which is the main drawback of the traditional sliding mode control. This strategy is robust in terms of load variations and system uncertainties.

The chattering effect being the main drawback that classical sliding model control exhibits, the main proposal in this work is to reduce it and, as a consequence, reduce high frequency oscillations.

In this paper, an Adaptive Sliding Mode Controller (ASMC) [32] is applied with a two-loop control approach with the purpose of extracting the maximum power from a PV panel under non ideal/constant conditions. The study uses an IPSM-based MPPT algorithm to generate the commanded reference voltages for the voltage control loop. This will be done by suitable definition of the sliding surface. The layout of the system to be controlled is built up by the interconnection of the PV panel and a DC load that receives power extracted from the panel by using a boost converter. The ASMC controller is derived based on the idea proposed in [33]. System stability is ensured by applying Lyapunov candidate function.

Simulation platforms used in this work are MATLAB/Simulink and PSIM. Whereas the boost converter, the PV panel, and the MPPT algorithm are implemented in PSIM, the voltage, lower level, and controller are deployed by using MATLAB/Simulink.

In order to evaluate the performance of the proposed PV operation configurations, we need to evaluate the capabilities for voltage following as well as extracted power. Results are to be compared with the ones obtained by a PID controller. The performance comparison is based on usual figures of merit such as steady state error, oscillations, etc. As the operational architecture is composed of two levels of operation (being the PID at the lower level), the comparison also includes two other options for the upper level. These two options are P&O and PSO as widely used MPPT algorithms.

This work follows previous studies proposed by the author in [34], where an integer order SMC controller was modelled for extraction of maximum power from PV. Classical SMC generally suffer from the problem of ‘chattering’, which is a very high frequency oscillation of the sliding variable around the sliding manifold. In this study, the authors have introduced an adaptive version of SMC that reduces the chattering phenomenon and limits high frequency oscillations that were present in [34]. Along with this, the authors have implemented two more MPPT algorithms (PSO, IPSM) with the proposed controller that was conducted in the previous studies [33,34] with only conventional P&O MPPT. It has been observed that the IPSM optimization method is computationally efficient and offers the best solution than the other optimization algorithms PSO and P&O. This study is developed to reduce the chattering effect and high frequency oscillations that were present in [34] behavior. The conducted methodology presented initially in [33] is used to nullify the chattering effect and improve tracking response and power losses to enhance overall efficiency of the stand-alone PV system, which is shown by estimating numerical analysis in form of overshoot, settling time, and losses.

The overall paper is organized as follows: in Section 2, interrelated work is deliberated. Section 3 presents the system model for this work and the derivation of proposed control scheme is shown. Simulation results are described in Section 4. Lastly, Section 5 sums up the conclusion and the possible future work.

## 2. Problem Formulation

Figure 1 shows the topology of the implemented work in this study. Stand-alone PV system is used which consists of a PV panel, DC-DC boost converter, a load and a control loop that produces PWM signal to the step-up converter for MPPT process. This work is established on the concepts published in [33], which apply the adaptive sliding mode technique to adjust the PV voltage and to

alleviate the chattering effect. The description of the work is explained in work published in [33] that guarantees the maximum power is produced successfully by the proposed control methodology.

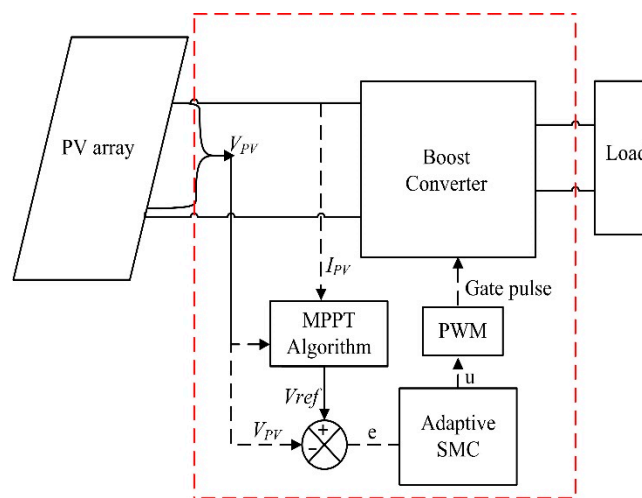


Figure 1. Block diagram of the system scheme based on adaptive sliding mode control.

### 3. System Model

The schematic circuit diagram of the PV system used in this study is appeared in Figure 2, which is made out of a PV module and a power electronic converter. A two-diode model representation of PV cell is chosen that involves identification of more system parameters and better proficiency. This representation provides more accurate output PV characteristic curves, i.e., I-V and P-V [35].

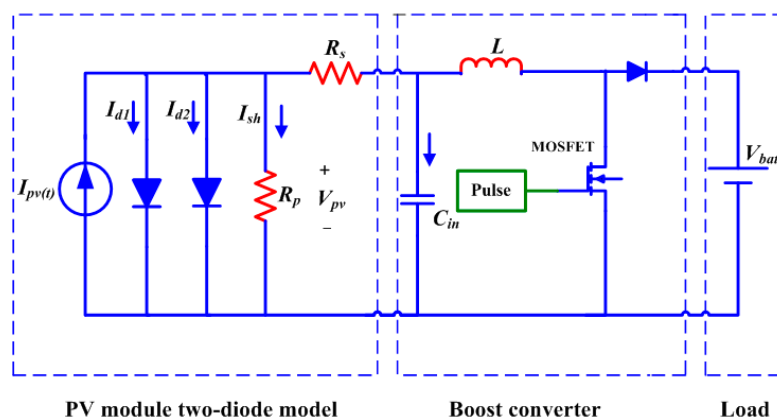


Figure 2. Circuit diagram the proposed PV system.

In order to appropriately operate the PV panel power extraction, a converter is needed. As shown in Figure 2, here we will use a DC–DC converter that operates between the panel and the load [36]. In this work, the boost converter will be utilized [34].

#### 3.1. MPPT Algorithms

##### 3.1.1. MPPT Algorithm Based on P&O

The P&O MPPT algorithm is based on managing either the voltage command or the boost converter input current. Subsequently, the measure of power converted from the panel is estimated. The P&O algorithm adopted methodology description is explained in [36], in which an integer order sliding mode controller had been proposed for the two-diode model-based PV system. The P&O MPPT algorithm had been used in [34] in order to be able to extract the maximum power from the panel

and providing the reference voltage to the sliding mode controller acting as a voltage loop controller. Here, the controller is modified by Adaptive SMC to address the chattering phenomenon that was present in [34]. The P&O algorithm flow diagram is shown in Figure 3, which is executed in PSIM simulation tools.

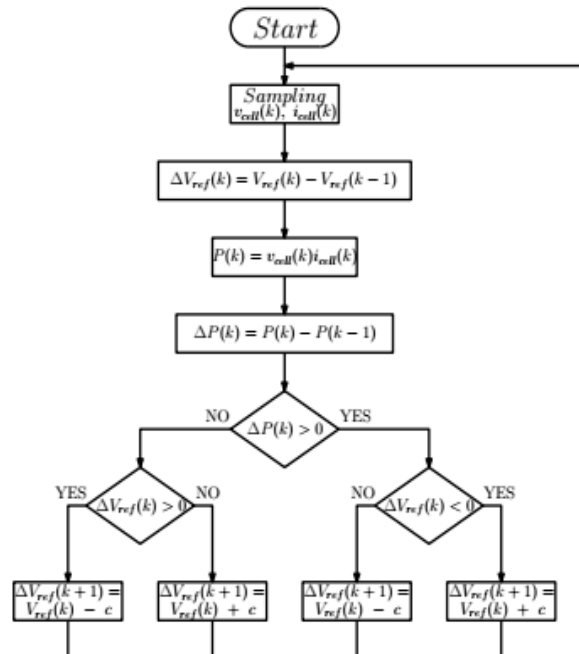


Figure 3. Perturb and observe (P&O) algorithm.

### 3.1.2. MPPT Algorithm Based on PSO

Particles Swarm Optimization (PSO) [34,37] algorithms are strategies based on a heuristic search that use a population, characterized with stochastic features, which are motivated by swarms. Each one of such particles constitutes a candidate solution. PSO calculations produce new particles positions and features on the basis of its interaction with the rest. For example, for what matters to the particle position, it is determined on the basis of particles in a superior situation. This superior situation, in our case study, corresponds to a reference voltage that generates a more efficient power conversion. As an iteration-based approach, once a particle with superior characteristics is found, the rest of the particles will be affected by this. This winning particle will constitute the output of the algorithm. The flow diagram of the PSO algorithm is depicted in Figure 4.

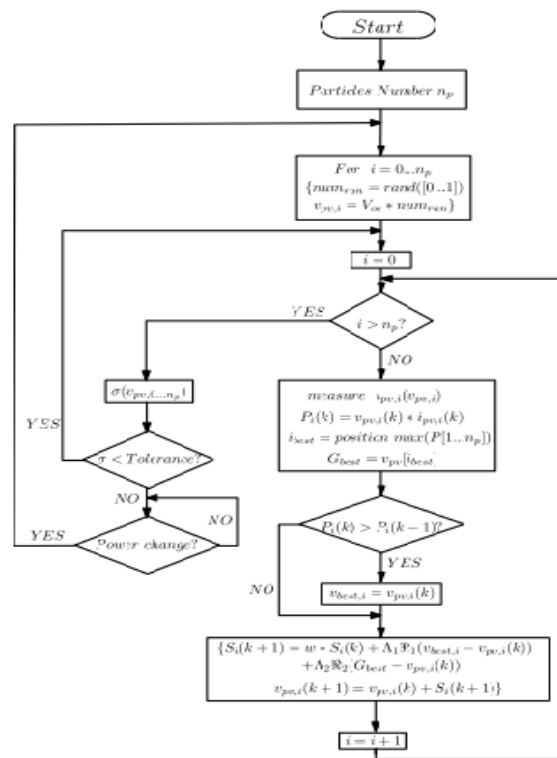


Figure 4. Particle Swarm Optimization (PSO) algorithm.

### 3.1.3. MPPT Algorithm Based on IPSM

In this case, IPSM is an improvement with respect to the Pattern Search Method (PSM) from [38]. Pattern Search algorithms are defined along two main constitutive parts: first, an arrangement of mesh definitions and, second, a list of polling conditions. Every component of the mesh is a solution candidate. Pattern Searches methods are also iterative methods. Therefore, at each iteration, the meshes move towards the best position, according to a convergence condition. In this case, the search is actualized with respect to the one in [17] by also introducing a search at the adjoining members to the one that is defined as with the best position. This update, for the case at hand, introduces the possibility to guarantee appropriate convergence even in cases of radiation or partial shading. Figure 5 shows the algorithm as applied here for power conversion of the PV panel.

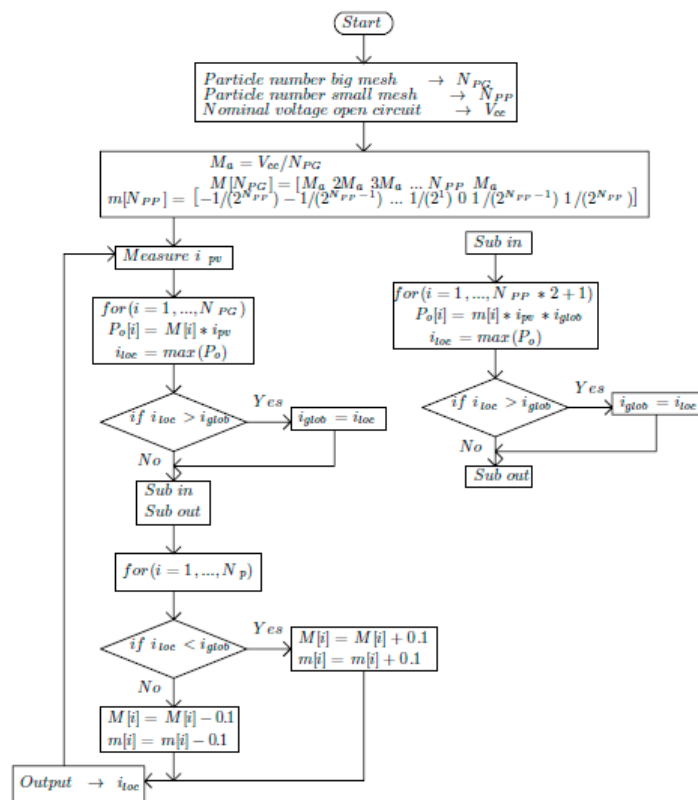


Figure 5. Proposed IPSM algorithm.

### 3.2. Control Scheme

#### Control Law

The work is based on the published work in [33,34]. Figure 6 shows the schematic circuital representation of the proposed adaptive SMC controller PV system. The operation of the work has been described in detail in [34]. Therefore, referring to the published work [33] the dynamics of the DC–DC boost converter is given by:

$$I_{cin} = (C_{in} + \Delta C_{in}) \frac{dV_{pv}}{dt} = I_{pv} - I_L \tag{1}$$

$$V_L = (L + \Delta L) \frac{dI_L}{dt} = V_{PV} - V_b(1 - u) \tag{2}$$

The above parameters definition can be read in [34].  $\Delta$  is the uncertainty term. Rearranging Equations (1) and (2) we have

$$\dot{V}_{PV} = -\frac{I_L}{C_{in} + \Delta C_{in}} + \frac{I_{PV}}{C_{in} + \Delta C_{in}} \tag{3}$$

$$\dot{I}_L = \frac{V_{PV}}{L + \Delta L} - \frac{V_b}{L + \Delta L} + \frac{V_b}{L + \Delta L} u \tag{4}$$

Equations (3) and (4) can be written in state space form as:

$$\begin{bmatrix} \dot{V}_{PV} \\ \dot{I}_L \end{bmatrix} = \begin{bmatrix} 0 & -1 \\ 1 & 0 \end{bmatrix} \frac{1}{C_{in} + \Delta C_{in}} \begin{bmatrix} V_{PV} \\ I_L \end{bmatrix} + \begin{bmatrix} \frac{I_{PV}}{C_{in} + \Delta C_{in}} & 0 \\ \frac{-V_b}{L + \Delta L} & 0 \end{bmatrix} \begin{bmatrix} 1 \\ 0 \end{bmatrix} + \begin{bmatrix} 0 \\ \frac{V_b}{L + \Delta L} \end{bmatrix} u \tag{5}$$

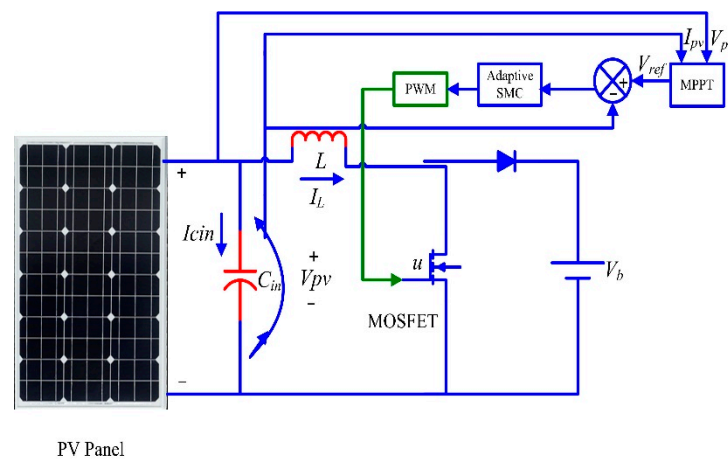


Figure 6. System circuitual scheme based on Adaptive sliding mode control.

Equation (5) can be re-written in generalized form as:

$$\dot{X} = f(X, t) + J(X, t) + h(X, t) u + \Delta f(X, t) + \Delta J(X, t) + \Delta h(X, t) u + d(X, t) \quad (6)$$

All above shown parameters are defined in published work [33]. where,

$$f(X, t) = \begin{bmatrix} 0 & -1 \\ \frac{1}{L} & \frac{C_{in}}{0} \end{bmatrix} \quad (7)$$

$$J(X, t) = \begin{bmatrix} \frac{I_{PV}}{C_{in}} & 0 \\ -\frac{V_b}{L} & 0 \end{bmatrix} \quad (8)$$

$$h(X, t) = \begin{bmatrix} 0 \\ \frac{V_b}{L} \end{bmatrix} \quad (9)$$

$$\Delta f(X, t) = \begin{bmatrix} 0 & -1 \\ \frac{1}{\Delta L} & \frac{\Delta C_{in}}{0} \end{bmatrix} \quad (10)$$

$$\Delta J(X, t) = \begin{bmatrix} \frac{I_{PV}}{\Delta C_{in}} & 0 \\ -\frac{V_b}{\Delta L} & 0 \end{bmatrix} \quad (11)$$

$$\Delta h(X, t) = \begin{bmatrix} 0 \\ \frac{V_b}{\Delta L} \end{bmatrix} \quad (12)$$

Equation (6) can also be given the following generic form

$$\dot{X} = f(X, t) + J(X, t) + h(X, t) u + D(X, t) \quad (13)$$

where

$$D(X, t) = \Delta f(X, t) + \Delta J(X, t) + \Delta h(X, t) u + d(X, t) \quad (14)$$



The MPPT algorithm will generate a command signal for the lower level control loop. Such command is given by:

$$X_d = \begin{bmatrix} x_d & \dot{x}_d \end{bmatrix}^T = \begin{bmatrix} V_{PV-ref} & \dot{V}_{PV-ref} \end{bmatrix}^T \quad (15)$$

The tracking error can be defined as:

$$\begin{cases} e_1 = x_1 - x_d \\ e_2 = \dot{e}_1 \\ e_2 = x_2 - \dot{x}_d \\ \dot{e}_2 = \dot{x}_2 - \ddot{x}_d \end{cases} \quad (16)$$

The sliding surface can be chosen as:

$$s = k_1 e_1 + e_2 \quad (17)$$

here  $k_1 > 0$  is the design parameter. Differentiating Equation (17) on both sides

$$\dot{s} = k_1 \dot{e}_1 + \dot{e}_2 \quad (18)$$

By combining (13) and (18) one can obtain

$$\dot{s} = c_1 \dot{e}_2 + f(X, t) + J(X, t) + h(X, t)u + D(X, t) - \ddot{x}_d \quad (19)$$

The controller that achieves the desired output is:

$$\begin{cases} u = u_a + u_s \\ u_a = h(X, t)^{-1} [\ddot{x}_d - f(X, t) - J(X, t) - c_1 \dot{e}_2 - \hat{D}(X, t)] \\ u_s = -h(X, t)^{-1} k_s \text{sgn}(s) \end{cases} \quad (20)$$

The obtained derived parameters definition can be read in [33]. Signum function  $\text{sgn}(\cdot)$  can be defined as:

$$\text{sgn}(s) = \begin{cases} +1 & \text{if } s > 0 \\ 0 & \text{if } s = 0 \\ -1 & \text{if } s < 0 \end{cases} \quad (21)$$

The stability of the proposed control scheme has been proved and checked in [33] by the Lyapunov candidate function. It has been analyzed that the close loop system is stable.

#### 4. Simulation Results and Discussion

In this section, the results for each one of the three MPPT implemented algorithms are shown. First of all, the description of the irradiance experiment as well as parameters for the PV system as well as MPPT and controller parameters are provided. Next, a separate subsection for each MPPT algorithm provides the corresponding results and evaluation. The section ends with a comparative summary.

MATLAB/Simulink is utilized to model and perform simulations of the proposed controllers' methods. The simulations of PV module and power electronic converter with MPPT controller are performed in PSIM (PowerSim). To perform co-simulations between MATLAB/Simulink and PSIM, Simcoupler is used. The parameters of PV that are utilized in this study can be found in Table 1. In PSIM physical model [39] of a PV board is available that is used in simulations, with parameters comparing to the PV module of type MXS-60 [40].

**Table 1.** Parameters of PV Array [37].

Symbol	Parameter	Value
$I_{SC}$	Short-circuit current	3.8 A
$V_{OC}$	Open-circuit voltage	21.1 V
$I_{mp}$	Maximum panel current	3.5 A
$V_{PV}$	Maximum panel voltage	17.1 V
$I_{S1} = I_{S2}$	Saturation currents	$4.704 \times 10^{-10}$
$I_{PV}$	Panel current	3.8 A
$R_{sh}$	Shunt resistance	176.4 $\Omega$
$R_s$	Series resistance	0.35 $\Omega$ .

Table 2 provides the parameters of converter and controller that are used in this work. MATLAB optimization tools are used to obtain the design parameters of controllers, which are displayed additionally in this table. The experimental conditions that will be simulated consists of an initial irradiance step of 1000 W/m<sup>2</sup> followed by a 50% decrease of irradiance. The working temperature is 25 °C.

**Table 2.** Parameters of controller, converter and MPPT.

Parameters	Value
L	22 $\mu$ F
C	100 $\mu$ F
$V_o$	24 V
$f_{sw0}$ (controller)	49.2 kHz
$K_p$	0.1
$K_I$	50
$K_d$	0.1
$K_1$	4.3
$K_A$	55.5
$T_a$	400 $\mu$ s
$\Delta V_o$	1 V (P&O)
$\Delta V_o$	0.2 V (40 p.)
$\Delta V_o$	0.8 V (10 p.)
LPF	20 kHz

#### 4.1. Simulation Results

##### 4.1.1. Response Using P&O

In this section we will compare the performance of the ASMC with that one of the PID controller. Both operating under the voltage reference generation by using P&O. PID controller tuning parameters have been obtained by using MATLAB/Simulink optimization tools. To show the performance of the proposed chattering-free ASMC controller, first, the conventional technique PID with P&O MPPT is compared with the proposed ASMC controller with P&O under the same system parameters and environmental parameters. Figure 7a–d shows the comparative behavior of both controllers using P&O MPPT with a P&O perturbation amplitude of 1 V. The output of P&O MPPT is a voltage reference signal that is supposed to be tracked by the PID controller to ensure tracking error as close as possible to zero. Figure 7a is the PV panel voltage, which is tracked by controller with reference voltage.

$V_{pv}$  successfully tracks  $V_{ref}$ . The PV voltage of PID deviates from  $V_{ref}$  while there is no deviation in the proposed controller PV voltage.

The tracking error comparative plot of PID and ASMC with P&O is shown in Figure 7b. There are high ripples and oscillations in PID tracking error behavior and fewer oscillations in ASMC. The implemented controller plainly overtakes the conventional controller with slight oscillation. PV panel output power curve is shown in Figure 7c. From power curve it can be seen that MPP is achieved successfully and the controllers track the reference voltage in the voltage curve but displays large ripples in the voltage waveform along with an overshoot in PID. It is clear that MPP is achieved by ASMC with reduced oscillations compared to PID. The results that are obtained by using ASMC are free of high frequency oscillations. Figure 7d depicts performance index IAE (Integral Absolute Error) of the PV system. The performance of the proposed controller has been verified based on this performance index.

As a resume quantitative comparison, Table 3 shows the different considered figures of merit. It can be observed that the performance has been improved by using the ASMC.

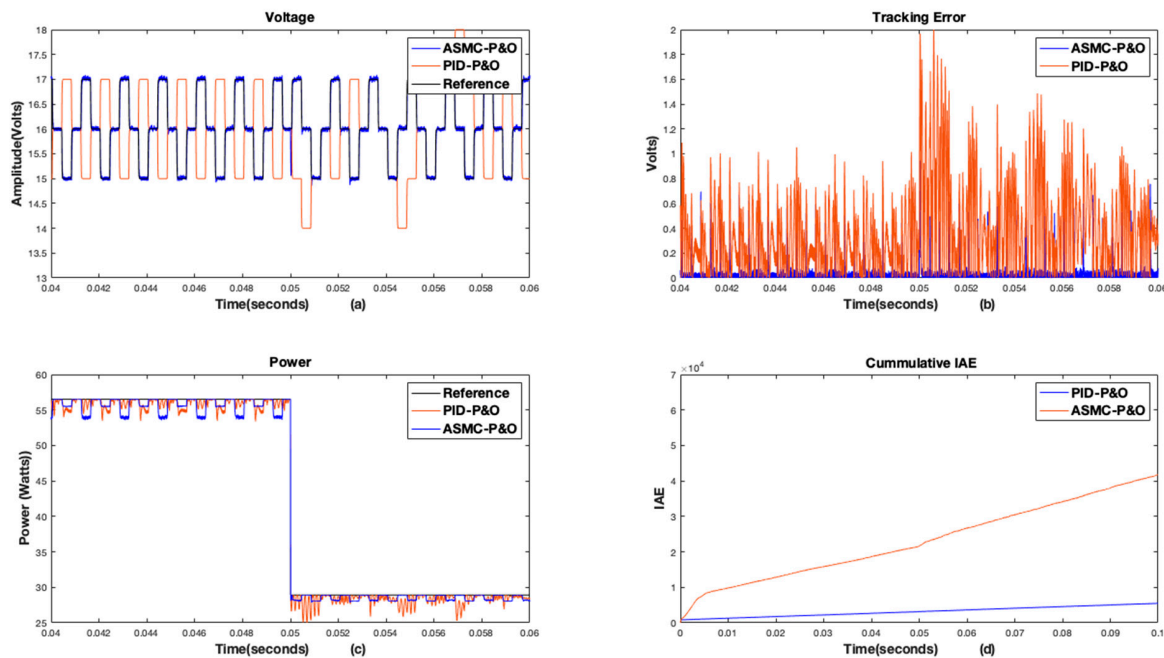


**Figure 7.** PID & ASMC based on P&O MPPT (a) Profile of the PV panel voltage (b) Tracking response (c) Profile of the PV power extraction (d) IAE.

**Table 3.** Performance characteristics of the conventional controller and the proposed ASMC controller based on P&O MPPT.

Controller	Over/Undershoot (%)	Settling Time (Second)	Power Losses (Watt)
PID	2.8	5.3 ms	3.2
ASMC	0.6	0.15 ms	0.68

#### 4.1.2. Response Using PSO

The combined response using conventional controller and the proposed ASMC controller based on PSO MPPT can be seen in Figures 8a–d and 9a–d. As a stochastic algorithm, PSO does not always guarantee the same exact location for the best positioned particle (optimal solution). Therefore, two sets of 10 simulations each has been conducted. A first simulation set using 10 particles and a second one using 40 particles.

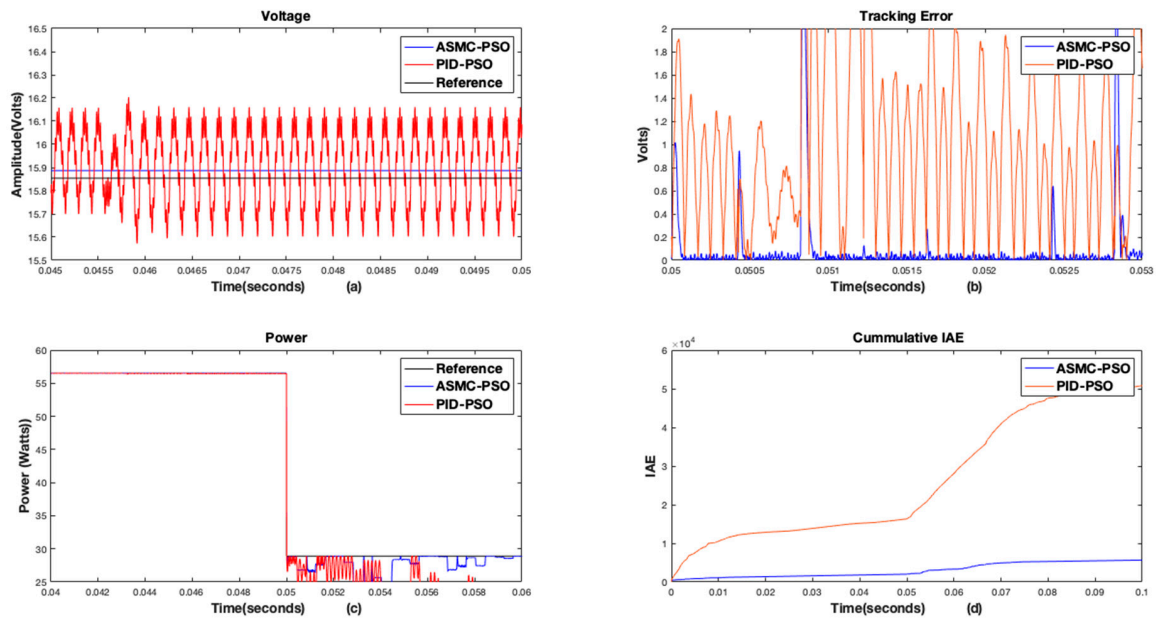


**Figure 8.** PID & ASMC based in PSO MPPT with 10 particles (a) Profile of the PV panel voltage. (b) Tracking response (c) Profile of the PV power extraction (d) IAE.

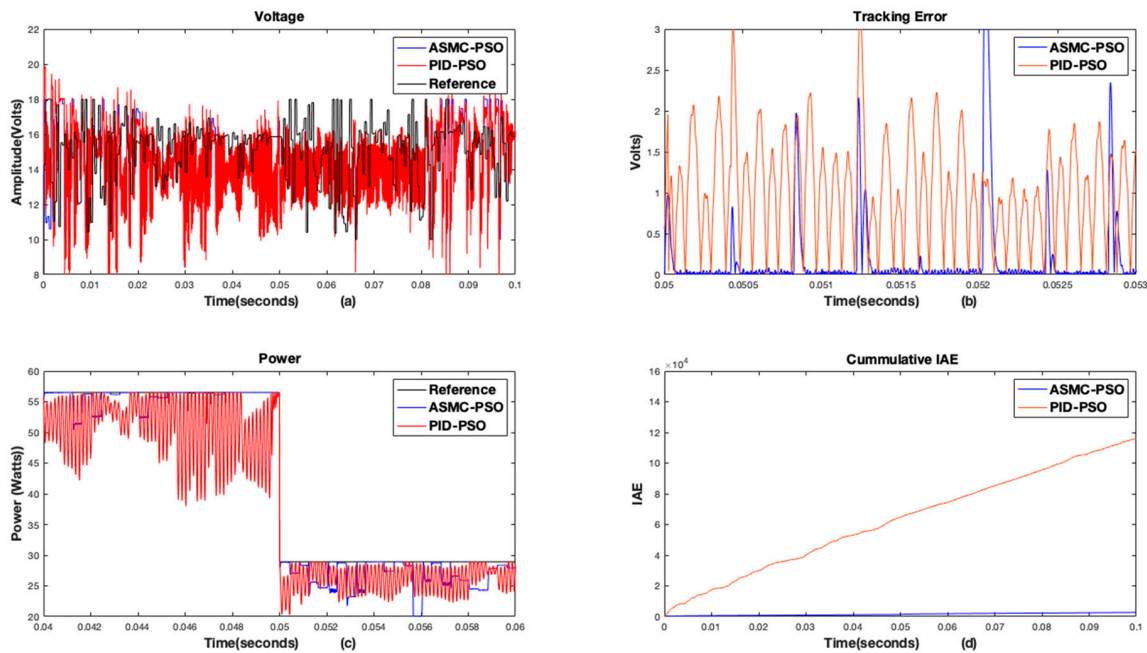


**Figure 9.** PID & ASMC based in PSO MPPT with 40 particles (a) Profile of the PV panel voltage. (b) Tracking response (c) Profile of the PV power extraction (d) IAE.

From PSO with 10 particles comparative plot, it can be observed that the controllers track the reference  $V_{ref}$  in the voltage curves in Figure 8a, the panel voltage is tracked by the controller with the reference voltage  $V_{pv-ref}$ . The tracking error response that is shown in Figure 8b with less oscillations and ripples as compared to P&O MPPT-based results and MPP is achieved in the power curves in Figure 8c. PSO with 10 particles shows the average response, and the algorithm reached the MPP before the simulation ended. However, the behavior using ASMC shows limited oscillations and less ripples in comparison of PID.

On the other hand, the response of PSO algorithm with 40 particles in Figure 9a–c never reached the steady state unlike the response based on PSO with 10 particles and always keeps moving around

the search-space. However, with adaptive SMC the oscillations reduced in the performance of PSO with 40 particles, which are significant in PID. As a result, it can be seen that, as a MPPT algorithm, PSO generated reference voltages with large oscillations, therefore energy losses, and, in some situations, difficulties to appropriately reach the steady state. The performance index of PV system (IAE) as shown in Figures 8d and 9d validate the effectiveness of the proposed control scheme with PSO MPPT. The performance characteristic parameters with PSO 10 particles is given in Table 4 and with PSO 40 particles is shown in Table 5.

**Table 4.** Performance characteristics of the conventional controller and the proposed ASMC controller based on PSO 10 particles.

Controller	Over/Undershoot (%)	Settling Time (Second)	Power Losses (Watt)
PID	8	80 ms	6
ASMC	0.85	2.8 ms	0.95

**Table 5.** Performance characteristics of the conventional controller and the proposed ASMC controller based on PSO 40 particles.

Controller	Over/Undershoot (%)	Settling Time (Second)	Power Losses (Watt)
PID	10	120 ms	7.8
ASMC	1	3 ms	1.2

#### 4.1.3. Response Using Improved PSM

In this section, the MMPT algorithm based on Improved PSM will be tested. As in the preceding section, because the algorithm is of stochastic nature, two sets of 10 simulations each will be pursued; one with 10 models and a second one with 40 models. Results are shown in Figures 10a–d and 11a–d, respectively. IPSM with 10 and 40 models converge faster than PSO with 10 and 40 particles. The perturbation amplitude is greater when the number of models will be low or vice versa to reach to the optimal solution. It is clear from the comparative plots given below that the proposed ASMC controller based on IPSM MPPT has negligible ripples and no deviation from MPP in obtained voltage and power curves.

The PV panel voltage curves Figures 10a and 11a track the reference voltage; PID voltage curve deviates from reference voltage and has great oscillations, while there is negligible deviation in the adaptive SMC voltage curve from reference. The PV array output power are shown in Figures 10b and 11b following the reference power. The main feature to highlight from the IPSM-based MPPT algorithm in comparison with the previously presented ones, is that it takes some more time to get the MPP but it guarantees to reach it. Furthermore, it exhibits less power energy losses than the PSO. The tracking error comparative plots are shown in Figures 10c and 11c, which highlight lower oscillations.

From the voltage curves (Figures 10a and 11a) the conventional controller tracks the panel voltage successfully with reference voltage. The power curves achieved the MPP in Figures 10c and 11c. The tracking error curves (Figures 10b and 11b) show minimized tracking error behavior as compared to PSO MPPT tracking response

In Figures 10d and 11d the performance index IAE of the PV system is depicted. This aggregated index confirms that this approach provides better performance than the other implemented MPPT techniques. In this manner, the validation of the chattering-free and robustness of the proposed adaptive sliding mode controller based on IPSM MPPT under variable environmental conditions and uncertainties is validated by comparing its performance with conventional controller based on P&O and PSO MPPT algorithms. The performance characteristic parameters are shown in Tables 6 and 7, which describe the overshoot characteristic, response time, and power losses.

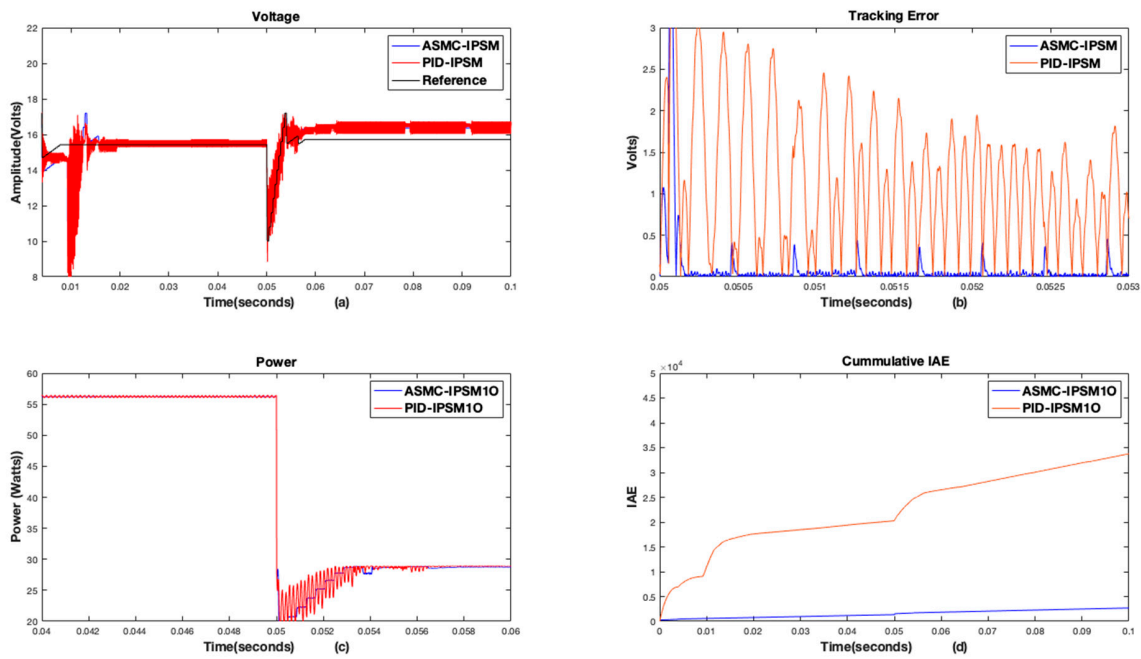


**Figure 10.** PID & ASMC based in IPISM MPPT with 10 particles (a) Profile of the PV panel voltage (b) Tracking response (c) Profile of the PV power extraction (d) IAE.

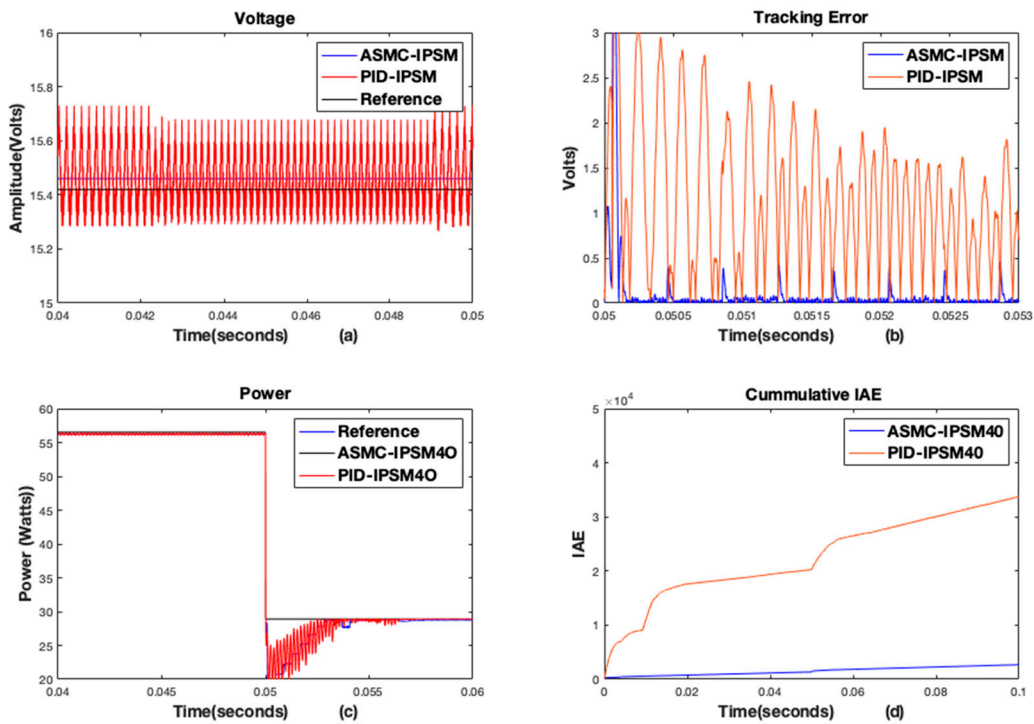


**Figure 11.** PID & ASMC based in IPISM. MPPT with 40 particles (a) Profile of the PV panel voltage (b) Tracking response (c) Profile of the PV power extraction (d) IAE.



**Table 6.** Performance characteristics of the conventional controller and the proposed ASMC controller based in IPSM with 10 models.

Controller	Over/Undershoot (%)	Settling Time (Second)	Power Losses (Watt)
PID	5	50 ms	4.8
ASMC	0.40	0.10 ms	0.54

**Table 7.** Performance characteristics of the conventional controller and the proposed ASMC controller based in IPSM with 40 models.

Controller	Over/Undershoot (%)	Settling Time (Second)	Power Losses (Watt)
PID	5.8	53 ms	5.2
ASMC	0.41	0.11 ms	0.59

#### 4.2. Discussion

From the previous three scenarios, the IPSM MPPT algorithm provides an overall satisfactory response. This improved approach may need some more time to get the MPP but it guarantees to reach it. Furthermore, it exhibits less energy losses than the other ones. The aggregated error index, IAE, shows that this technique is performing better than the ones based on P&O and PSO MPPT algorithms. Regarding the specific comparison with the other evolutive algorithm, PSO, IPSM with 10 and 40 particles converges faster than PSO with 10 and 40 particles. In addition, PSO-based results presents great oscillations, energy losses, and, in some cases, the algorithm cannot obtain the steady state. Therefore, confirming the proposed adaptive sliding mode controller based on IPSM MPPT is better performing by comparing its performance with conventional controller based on P&O and PSO MPPT algorithms.

### 5. Conclusions

In the present work, the design of a non-linear adaptive sliding mode controller (ASMC) based on a mathematical model of a boost converter has been derived for a stand-alone photovoltaic system to address the chattering phenomenon.

An IPSM optimization algorithm is used to generate the reference voltage for the proposed controller. Comparison with two other optimization algorithms, namely, P&O and PSO with IPSM for MPPT has been conducted. The presented control scheme is investigated in simulations under variable irradiance and uncertainties in the system parameters.

From the simulation results, we conclude that the ASMC controller with P&O MPPT presents constant oscillations around MPP, power losses, and overshoots, although it is the fastest one to obtain the MPP. On the other side, the ASMC controller with PSO MPPT presents great oscillations, the greatest energy losses, and, in some cases, it cannot obtain the MPP. Besides, the ASMC controller with IPSM MPPT is slower to obtain the MPP but presents lower energy losses versus adequate settling time in comparison with the other two algorithms.

Clear advantages of the tested optimization based MPPT algorithms over traditional P&O have been shown. In both cases, 10 and 40 particle optimizations have been conducted. Regarding IPSM, as shown in Tables 6 and 7, ASMC results are similar in both cases (10 and 40 particles) and superior in speed of response and power losses to the PSO ones (IPSM shows to be two times faster and exhibits half the power losses). It is worth mentioning that, for the ASMC based P&O MPPT algorithm, it provides reasonable performance indicators, even aligned with the PSO based MPPT but even faster from the settling time point of view (see Tables 3–5). In the case of the IPSM, the settling time is greatly improved with respect to PSO and made overall better results with respect to the original P&O. IPSM, therefore, provides a good alternative to the MPPT algorithm.

The simulation results are further compared with a classical PID controller to show the robustness of the developed adaptive SMC control scheme. The results obtain using ASMC controller in comparison with PID controller limits the chattering phenomenon and overcomes the high frequency oscillations. As a next step, the authors look forward to an experimental validation of the results.

**Author Contributions:** H.G.A., R.V.A. conceived and designed the experiments; H.G.A. performed the simulations; writing—review and editing, R.V.A.; supervision, R.V.A.; H.G.A wrote the paper. All authors have read and agreed to the published version of the manuscript.

**Funding:** This research was financed by the Spanish MINECO/FEDER grant DPI 2016-77271 and the APC was supported from this project.

**Acknowledgments:** This study was funded by the Spanish MINECO/FEDER grant DPI 2016-77271. The authors thank to National University of Science and Technology Islamabad, Pakistan for financial support during the completion of this research work.

**Conflicts of Interest:** The authors declare no conflict of interest.

## References

1. Ekins, P.; Bradshaw, M.J.; Watson, J. *Global Energy: Issues, Potentials, and Policy Implications*; Oxford University Press: Oxford, UK, 2015.
2. Ram, J.P.; Babu, T.S.; Rajasekar, N. A comprehensive review on solar PV maximum power point tracking techniques. *Renew. Sustain. Energy Rev.* **2017**, *67*, 826–847. [[CrossRef](#)]
3. Karami, N.; Moubayed, N.; Outbib, R. General review and classification of different MPPT Techniques. *Renew. Sustain. Energy Rev.* **2017**, *68*, 1–18. [[CrossRef](#)]
4. Elbaset, A.A.; Khaled, M.; Ali, H.; Sattar, M.A.-E. Implementation of a modified perturb and observe maximum power point tracking algorithm for photovoltaic system using an embedded microcontroller. *IET Renew. Power Gener.* **2016**, *10*, 551–560. [[CrossRef](#)]
5. Tey, K.S.; Mekhilef, S. Modified Incremental Conductance Algorithm for Photovoltaic System Under Partial Shading Conditions and Load Variation. *IEEE Trans. Ind. Electron.* **2014**, *61*, 5384–5392. [[CrossRef](#)]
6. Titri, S.; Larbes, C.; Toumi, K.Y.; Benatchba, K. A new MPPT controller based on the Ant colony optimization algorithm for Photovoltaic systems under partial shading conditions. *Appl. Soft Comput. J.* **2017**, *58*, 465–479. [[CrossRef](#)]
7. Ali, A.; Almutairi, K.; Malik, M.Z.; Irshad, K.; Tirth, V.; Algarni, S.; Zahir, H.; Islam, S.; Shafiullah, M.; Shukla, N.K. Review of Online and Soft Computing Maximum Power Point Tracking Techniques under Non-Uniform Solar Irradiation Conditions. *Energies* **2020**, *13*, 3256. [[CrossRef](#)]
8. Bahgat, A.; Helwa, N.; Ahmad, G.; El Shenawy, E. Maximum power point tracking controller for PV systems using neural networks. *Renew. Energy* **2005**, *30*, 1257–1268. [[CrossRef](#)]
9. Sampaio, L.P.; Da Rocha, M.V.; Da Silva, S.A.O.; De Freitas, M.H.T.; De Freitas, M.T. Comparative analysis of MPPT algorithms bio-inspired by grey wolves employing a feed-forward control loop in a three-phase grid-connected photovoltaic system. *IET Renew. Power Gener.* **2019**, *13*, 1379–1390. [[CrossRef](#)]
10. Purnama, I.; Lo, Y.-K.; Chiu, H.-J. *A Fuzzy Control Maximum Power Point Tracking Photovoltaic System, Proceedings of the 2011 IEEE International Conference on Fuzzy Systems, Taipei, Taiwan, 27–30 June 2011*; Institute of Electrical and Electronics Engineers: Piscataway, NJ, USA, 2011; pp. 2432–2439.
11. Elobaid, L.M.; Abdelsalam, A.K.; Zakzouk, E.E. Artificial neural network-based photovoltaic maximum power point tracking techniques: A survey. *IET Renew. Power Gener.* **2015**, *9*, 1043–1063. [[CrossRef](#)]
12. Kulaksız, A.A.; Akkaya, R. A genetic algorithm optimized ANN-based MPPT algorithm for a stand-alone PV system with induction motor drive. *Sol. Energy* **2012**, *86*, 2366–2375. [[CrossRef](#)]
13. Ferdiansyah, I.; Sutedjo, S.; Qudsi, O.A.; Ramadhan, A.N. Implementation of Maximum Power Point Tracking on Solar Panels using Cuckoo Search Algorithm Method. In *Proceedings of the 2nd International Conference on Applied Information Technology and Innovation, Denpasar, Bali, 21–22 September 2019*; pp. 88–92. [[CrossRef](#)]
14. Besheer, A.H.; Adly, M. Ant Colony System Based Pi Maximum Power Point Tracking for Stand Alone Photovoltaic System. In *Proceedings of the 2012 IEEE International Conference on Industrial Technology, Athens, Greece, 19–21 March 2012*; Institute of Electrical and Electronics Engineers: Piscataway, NJ, USA, 2012; pp. 693–698.



15. Renaudineau, H.; Donatantonio, F.; Fontchastagner, J.; Petrone, G.; Spagnuolo, G.; Martin, J.-P.; Pierfederici, S. A PSO-Based Global MPPT Technique for Distributed PV Power Generation. *IEEE Trans. Ind. Electron.* **2014**, *62*, 1047–1058. [[CrossRef](#)]
16. Tajuddin, M.F.N.; Ayob, S.M.; Salam, Z.; Saad, M.S. Evolutionary based maximum power point tracking technique using differential evolution algorithm. *Energy Build.* **2013**, *67*, 245–252. [[CrossRef](#)]
17. Javed, M.Y.; Murtaza, A.F.; Ling, Q.; Qamar, S.; Gulzar, M.M.; Javed, Y. A novel MPPT design using generalized pattern search for partial shading. *Energy Build.* **2016**, *133*, 59–69. [[CrossRef](#)]
18. Audet, C. Convergence Results for Generalized Pattern Search Algorithms are Tight. *Optim. Eng.* **2004**, *5*, 101–122. [[CrossRef](#)]
19. Veerapen, S.; Wen, H.; Du, Y. Design of a novel MPPT algorithm based on the two stage searching method for PV systems under partial shading. In Proceedings of the 3rd International Future Energy Electronics Conference and ECCE Asia, Kaohsiung, Taiwan, 3–7 June 2017; pp. 1494–1498. [[CrossRef](#)]
20. Abdelrassoul, R.; Ali, Y.; Zaghoul, M.S. Genetic Algorithm-Optimized PID Controller for Better Performance of PV System. In Proceedings of the 2016 World Symposium on Computer Applications and Research, Cairo, Egypt, 12–14 March 2016; pp. 18–22.
21. Ali, A.I.M.; Mohamed, E.E.M.; Youssef, A.R. MPPT algorithm for grid-connected photovoltaic generation systems via model predictive controller. In Proceedings of the 19th International Middle-East Power Systems Conference, Cairo, Egypt, 19–21 December 2018; pp. 895–900.
22. Guler, N.; Irmak, E. MPPT based model predictive control of grid connected inverter for PV system. In Proceedings of the 8th International Conference of Renewable Energy Research and Applications, Brasov Romania, 3–6 November 2019; pp. 982–986.
23. Khanna, R.; Zhang, Q.; Stanchina, W.E.; Reed, G.F.; Mao, Z.-H. Maximum Power Point Tracking Using Model Reference Adaptive Control. *IEEE Trans. Power Electron.* **2013**, *29*, 1490–1499. [[CrossRef](#)]
24. Chavarria, J.; Biel, D.; Guinjoan, F.; Meza, C.; Negroni, J.J. Energy-Balance Control of PV Cascaded Multilevel Grid-Connected Inverters Under Level-Shifted and Phase-Shifted PWMs. *IEEE Trans. Ind. Electron.* **2012**, *60*, 98–111. [[CrossRef](#)]
25. Iftikhar, R.; Ahmad, I.; Arsalan, M.; Naz, N.; Ali, N.; Armghan, H. MPPT for Photovoltaic System Using Nonlinear Controller. *Int. J. Photoenergy* **2018**, *2018*, 1–11. [[CrossRef](#)]
26. Chaibi, Y.; Salhi, M.; El-Jouni, A. Sliding mode controllers for standalone PV systems: Modeling and approach of control. *Int. J. Photoenergy* **2019**, *2019*. [[CrossRef](#)]
27. Ahmad, F.F.; Ghenai, C.; Hamid, A.K.; Bettayeb, M. Application of sliding mode control for maximum power point tracking of solar photovoltaic systems: A comprehensive review. *Annu. Rev. Control.* **2020**, *49*, 173–196. [[CrossRef](#)]
28. Bianconi, E.; Calvente, J.; Giral, R.; Petrone, G.; Paja, C.A.R.; Spagnuolo, G.; Vitelli, M. A Fast Current-Based Mpppt Technique Based on Sliding Mode Control. In Proceedings of the 2011 IEEE International Symposium on Industrial Electronics, Gdansk, Poland, 27–30 June 2011; pp. 59–64. [[CrossRef](#)]
29. Chu, C.-C.; Chen, C.-L. Robust maximum power point tracking method for photovoltaic cells: A sliding mode control approach. *Sol. Energy* **2009**, *83*, 1370–1378. [[CrossRef](#)]
30. Kchaou, A.; Naamane, A.; Koubaa, Y.; M'Sirdi, N. Second order sliding mode-based MPPT control for photovoltaic applications. *Sol. Energy* **2017**, *155*, 758–769. [[CrossRef](#)]
31. Mojallizadeh, M.R.; Badamchizadeh, M.; Khanmohammadi, S.; Sabahi, M. Designing a new robust sliding mode controller for maximum power point tracking of photovoltaic cells. *Sol. Energy* **2016**, *132*, 538–546. [[CrossRef](#)]
32. Kchaou, A.; Ayadi, A.; Naamane, A.; M'Sirdi, N.; Koubaa, Y. An Adaptive Sliding Mode Control based Maximum power point tracking method for a PV stand-alone system. In Proceedings of the 6th International Conference on Systems and Control, Batna, Algeria, 7–9 May 2017; pp. 69–74.
33. Ali, H.G.; Vilanova, R.; Pelez-Restrepo, J. Perturb & Observe based Adaptive Sliding Mode MPPT Control of Solar Photovoltaic System. In Proceedings of the 2020 IEEE International Conference on Environment and Electrical Engineering, Madrid, Spain, 9–12 June 2020; pp. 1–6.
34. Ali, H.G.; Vilanova, R.; Herrera, J.; Tobón, A.; Peláez-Restrepo, J. Non-Linear Sliding Mode Controller for Photovoltaic Panels with Maximum Power Point Tracking. *Process* **2020**, *8*, 108. [[CrossRef](#)]
35. Babu, T.S.; Ram, J.P.; Sangeetha, K.; Laudani, A.; Rajasekar, N. Parameter extraction of two diode solar PV model using Fireworks algorithm. *Sol. Energy* **2016**, *140*, 265–276. [[CrossRef](#)]

36. Hina; Noor, A.; Abbas, M.; Karimov, K.S. Non-inductive DC-DC regulated boost converter as battery charger for photovoltaic installation. In Proceedings of the 2015 Power Generation System and Renewable Energy Technologies, Islamabad, Pakistan, 10–11 June 2015; pp. 1–4. [[CrossRef](#)]
37. Salam, Z.; Ahmed, J.; Merugu, B.S. The application of soft computing methods for MPPT of PV system: A technological and status review. *Appl. Energy* **2013**, *107*, 135–148. [[CrossRef](#)]
38. Soon, J.J.; Low, K.-S. Photovoltaic Model Identification Using Particle Swarm Optimization With Inverse Barrier Constraint. *IEEE Trans. Power Electron.* **2012**, *27*, 3975–3983. [[CrossRef](#)]
39. Koessler, E.; Almomani, A. Hybrid particle swarm optimization and pattern search algorithm. *Optim. Eng.* **2020**, 1–17. [[CrossRef](#)]
40. PSIM Tutorial: How to Use Solar Module Physical Model. Available online: <https://powersimtech.com/drive/uploads/2016/04/Tutorial-Solar-Module-physical-model.pdf> (accessed on 1 April 2016).

**Publisher’s Note:** MDPI stays neutral with regard to jurisdictional claims in published maps and institutional affiliations.



© 2020 by the authors. Licensee MDPI, Basel, Switzerland. This article is an open access article distributed under the terms and conditions of the Creative Commons Attribution (CC BY) license (<http://creativecommons.org/licenses/by/4.0/>).